https://doi.org/10.5194/egusphere-2026-3910
Preprint. Discussion started: 21 July 2026

Chlorophyll–particle backscattering displacement reveals multiple deep chlorophyll maximum structures in the North Pacific

Taketo Hashioka[1] and Maki N. Aita[1]

[1]Research Institute for Global Change, Japan Agency for Marine-Earth Science and Technology, 2-15, Natsushima-cho, Yokosuka, Kanagawa, 237-0061, Japan

Correspondence to: Taketo Hashioka (hashioka@jamstec.go.jp)

Abstract. Subsurface chlorophyll-a (Chl) maxima are common features of stratified oceans, but a Chl maximum does not necessarily indicate a maximum in particle-associated optical structure. Here we use Biogeochemical-Argo (BGC-Argo) observations from the North Pacific during 2022–2025 to examine how the previously recognized separation between Chl maxima and particle-associated optical structure is expressed across a large set of vertically resolved in situ profiles. For 10,801 usable paired Chl and particulate backscattering at 700 nm (BBP700) profiles, we diagnosed the depths of the Chl DCM (deep chlorophyll maximum) and BBP700 maximum within the upper 300 dbar and classified profiles by their vertical displacement. Coupled profiles, in which the two maxima occurred within 25 dbar of each other, were the most frequent class and had median Chl DCM and BBP700 maximum depths of 52.5 and 47.5 dbar, respectively. In Chl deeper profiles, the Chl DCM was displaced downward relative to a shallower BBP700 maximum, consistent with a stronger contribution of photoacclimation or pigment adjustment to the Chl maximum. In Chl shallower profiles, a shallow Chl maximum coexisted with a deeper BBP700 maximum, demonstrating that Chl–BBP700 decoupling is not unidirectional. The three displacement classes showed coherent basin-scale spatial organization and distinct nitracline contexts, with the nitracline generally deeper than both optical maxima in Coupled and Chl deeper profiles, whereas Chl shallower profiles tended to show a deeper BBP700 maximum near the nitracline depth range. Together, these findings indicate that North Pacific Chl DCMs do not represent a single uniform vertical bio-optical structure. Instead, the previously recognized separation between Chl maxima and particle-associated optical structure is expressed in mature BGC-Argo observations as coherent vertical, spatial, and nitracline-related structures across the North Pacific.

1. Introduction

Chlorophyll-a (Chl) is widely used to describe phytoplankton distributions, but surface-focused observations do not resolve the vertical organization of Chl within the upper ocean. A large body of in situ observations has shown that subsurface Chl maxima are common features of stratified waters and vary systematically across ocean regions and environmental settings. These subsurface maxima provide an important view of upper-ocean bio-optical structure because their depth and prominence cannot be inferred from surface Chl alone. Global and regional syntheses have therefore emphasized the need to evaluate Chl vertical structure directly rather than treating the surface layer as representative of the water column (Cullen, 2015; Cornec et al., 2021; Yasunaka et al., 2022).

The interpretation of a Chl maximum is, however, not unique. Vertical changes in Chl can reflect changes in phytoplankton amount, changes in cellular pigment content associated with photoacclimation, or a combination of both. Simple theory and observational syntheses indicate that the depth of a Chl maximum need not coincide with the depth of the strongest particle-associated structure, particularly in stratified waters where light and nutrient gradients vary over similar depth ranges. Cornec et al. (2021) formalized this ambiguity for Biogeochemical-Argo (BGC-Argo) profiles by distinguishing Chl maxima associated with particle-backscattering structure from those more strongly associated with photoacclimation. Thus, a Chl DCM

https://doi.org/10.5194/egusphere-2026-3910
Preprint. Discussion started: 21 July 2026

(deep chlorophyll maximum) is best treated as an operational Chl feature whose relation to particle-associated structure must be evaluated explicitly (Fennel and Boss, 2003; Cullen, 2015; Cornec et al., 2021).

Particulate backscattering provides an independent bio-optical signal with which to examine this relationship. In BGC-Argo profiles, BBP700 represents an optical particle-backscattering signal that can be compared with the Chl profile without assuming a fixed conversion between Chl and particle-related optical structure. This distinction is important because global BGC-Argo analyses have shown that the relationship between particulate backscattering and Chl varies with vertical position, season, and oceanic regime. The depth relationship between the Chl DCM and the BBP700 maximum is therefore a useful observational diagnostic: it identifies whether the subsurface Chl maximum is vertically aligned with, deeper than, or shallower than the particle-backscattering maximum, rather than assuming that the two maxima are equivalent (Barbieux et al., 2018; Cornec et al., 2021).

BGC-Argo now provides vertically resolved, profile-based observations of Chl and particle backscattering over broad spatial domains. In the North Pacific, these observations can be used to examine Chl–backscattering relationships across subtropical, transition, and subarctic regimes within a single basin, where persistent subsurface Chl features create a wide range of vertical bio-optical structures. Recent assessments of BGC-Argo Chl observations in the western North Pacific further support the value of these profiles for examining regional upper-ocean Chl structure, while global BGC-Argo studies provide the broader context for Chl–backscattering comparisons. The North Pacific therefore provides a suitable setting for evaluating whether Chl DCMs and BBP700 maxima are vertically colocated or separated across contrasting hydrographic and biogeochemical conditions (Barbieux et al., 2018; Cornec et al., 2021; Yasunaka et al., 2022; Hayashida et al., 2025).

Despite these advances, the basin-scale organization of Chl–particle separation within the naturally variable North Pacific BGC-Argo profile population remains less clearly established. Rather than treating Chl–particle separation as a newly discovered phenomenon, we use the depth relationship between the Chl DCM and BBP700 maximum as an observational organizing axis to examine how the known ambiguity of Chl maxima is expressed in mature BGC-Argo observations. Using paired BGC-Argo Chl and BBP700 profiles, we quantify the depth difference between the Chl DCM and the BBP700 maximum, examine the resulting Coupled, Chl deeper, and Chl shallower configurations, and evaluate their vertical structures, spatial occurrence, and nitracline context across the North Pacific.

By doing so, this study provides an observational framework for interpreting Chl DCMs not as a single uniform proxy for particle abundance or biomass, but as a set of Chl–particle configurations in which the Chl maximum may either coincide with or be vertically separated from particle-backscattering structure. The significance of this framework is that it translates the known ambiguity of Chl maxima from profile-level interpretation into recurring vertical, spatial, and nutrient-context structures observed across the North Pacific BGC-Argo network.

2. Methods

2.1 BGC-Argo profile data and study domain

This study used BGC-Argo profile observations from the North Pacific during 2022–2025. The initial geographic window was defined as 0–65°N and 110–270°E using a 0–360° longitude convention. Profiles within this window were further restricted using a Pacific basin mask to retain the connected Pacific portion of the domain and exclude non-Pacific waters included by the rectangular longitude–latitude bounds. We refer to the resulting region as the North Pacific study domain.

This period was selected as the recent observational window in which paired Chl and BBP700 profiles were sufficiently available to evaluate the vertical relationship between Chl DCMs and BBP700 maxima at the basin scale. By combining observations over four years, the analysis was designed to avoid relying on a single year or a single seasonal snapshot, and to include profiles distributed across seasons and over a broad portion of the North Pacific study domain. Because BGC-Argo

https://doi.org/10.5194/egusphere-2026-3910
Preprint. Discussion started: 21 July 2026

sampling is not spatially uniform, the resulting maps and class fractions are interpreted as observational summaries of the available profile population rather than as spatially unbiased climatological fields.

The main paired Chl–BBP700 profile table contained 10,801 usable profiles. Each retained profile included geographic position, observation time, pressure, Chl, and BBP700 observations. In the retained paired-profile table, Chl and BBP700 were recorded from CHLA_ADJUSTED and BBP700_ADJUSTED, respectively. Pressure was used to define the vertical coordinate for the maximum-depth diagnostics described in Sect. 2.2.

Nitrate observations were not required for the main Chl–BBP700 displacement classification. When available, nitrate was used only for the nitracline-context analyses described in Sect. 2.6 and 2.7. Profiles without usable nitrate observations could therefore be included in the main Chl–BBP700 analyses but were excluded from the nitracline-context subset.

The main Chl–BBP700 analyses were restricted to profiles for which both Chl DCM depth and BBP700 maximum depth could be diagnosed. These usable paired profiles formed the common population for the displacement classification, composite vertical-structure analysis, spatial gridding, and class-fraction mapping described below.

2.2 Detection of Chl DCM and BBP700 maximum depths

Chl DCM and BBP700 maximum depths were diagnosed from paired Chl, BBP700, and pressure profiles. For each variable, only valid observations within 0–300 dbar were used. Profiles were binned onto 5 dbar pressure intervals, and the median value within each bin was calculated. Missing bins were not interpolated.

The binned Chl and BBP700 profiles were then smoothed using a centered five-bin rolling median with a minimum of one valid bin. The Chl DCM depth was defined as the bin-center depth of the maximum value on the smoothed binned Chl profile. The BBP700 maximum depth was defined analogously as the bin-center depth of the maximum value on the smoothed binned BBP700 profile.

Here, Chl DCM is used operationally to denote the depth of the maximum Chl signal within the upper 300 dbar. This definition includes shallow or near-subsurface maxima when they occurred within the search range and does not require the Chl maximum to be separated from the near-surface layer by a fixed depth threshold.

These diagnostic depths were used throughout the manuscript as the Chl DCM depth and the BBP700 maximum depth. BBP700 is interpreted here as an optical particle-backscattering signal rather than as a direct measure of biomass or particle concentration.

Profiles were retained for subsequent Chl–BBP700 displacement analysis only when both the Chl DCM depth and BBP700 maximum depth were successfully diagnosed. The vertical displacement between these two depths was then calculated as described in Sect. 2.3.

2.3 Chl–BBP700 vertical displacement and profile classification

For each usable paired Chl–BBP700 profile, the vertical displacement between the Chl DCM and the BBP700 maximum was quantified as

$$\Delta z = z(\text{Chl DCM}) - z(\text{BBP700 maximum}), \quad (1)$$

where z(Chl DCM) is the depth of the Chl DCM and z(BBP700 maximum) is the depth of the BBP700 maximum. Depths are treated as positive downward, so positive Δz indicates that the Chl DCM is deeper than the BBP700 maximum, whereas negative Δz indicates that the Chl DCM is shallower than the BBP700 maximum.

Profiles were classified into three displacement classes using fixed depth-difference thresholds. Profiles with $|\Delta z| \leq 25$ dbar were classified as Coupled, representing cases in which the Chl DCM and BBP700 maximum occurred at similar depths. Profiles with $\Delta z > 25$ dbar were classified as Chl deeper, and profiles with $\Delta z < -25$ dbar were classified as Chl shallower. These classes were used consistently in the profile-composite analysis, gridded class-fraction maps, and nitracline-context analysis.

https://doi.org/10.5194/egusphere-2026-3910
Preprint. Discussion started: 21 July 2026

The displacement classes were defined solely from the relative depths of the Chl DCM and BBP700 maximum. Nitracline depth was not used to define the Coupled, Chl deeper, or Chl shallower classes; it was diagnosed independently and used only as a post-classification nutrient-structure context.

2.4 Composite vertical-structure analysis

Composite Chl vertical structures were constructed separately for the Coupled, Chl deeper, and Chl shallower displacement classes. Within each class, profiles were sorted by Chl DCM depth and divided into 100 equal-rank bins. This rank-based approach was used to compare Chl vertical structure along the observed DCM-depth gradient within each displacement class without using fixed geographic or seasonal bins.

For each profile, Chl values were represented on the same pressure-bin framework used for the maximum-depth diagnostics and were normalized by the maximum Chl value of each profile before compositing. The composite Chl field was then calculated as the median profile-normalized Chl value within each pressure–rank bin. This normalization emphasizes relative vertical structure within profiles rather than differences in absolute Chl magnitude among profiles.

Bin-wise median Chl DCM and BBP700 maximum depths were overlaid on the composite Chl fields to summarize how the diagnosed optical maxima varied along the DCM-depth rank axis. These median-depth lines were calculated directly within rank bins and were not smoothed for display. Nitracline depth was not included in this composite analysis and was evaluated separately as described in Sect. 2.6 and 2.7.

2.5 Spatial gridding and class-fraction mapping

Spatial patterns of Chl DCM depth, BBP700 maximum depth, and Chl–BBP700 vertical displacement were summarized on a 2° × 2° latitude–longitude grid over the North Pacific study domain. For each grid cell, profile-level diagnostics were aggregated from profiles satisfying the paired Chl–BBP700 usability criteria. Median values were calculated for Chl DCM depth, BBP700 maximum depth, and vertical displacement.

To summarize the spatial distribution of displacement classes, the number of profiles in each class was counted within each 2° × 2° grid cell. Class fractions were calculated as the number of profiles in a given class divided by the total number of usable paired Chl–BBP700 profiles in that grid cell. The profile-count map summarized the spatial distribution of available observations. Gridded diagnostic maps and class-fraction maps were shown only for grid cells containing at least three usable paired profiles. Grid cells with fewer than three usable paired profiles were left blank in these summary maps.

No spatial interpolation or smoothing was applied to the gridded fields. The maps therefore represent cell-wise summaries of the available BGC-Argo profiles rather than interpolated continuous fields.

2.6 Nitracline depth diagnosis

Nitracline depth was diagnosed independently from the Chl–BBP700 displacement classification and was used only as a nutrient-structure context for profiles with usable nitrate observations. For profiles with nitrate measurements, nitrate was extracted from NITRATE_ADJUSTED whenever available; NITRATE was used only as a fallback when no adjusted nitrate variable was available. Pressure was treated similarly, using PRES_ADJUSTED preferentially and PRES otherwise.

For each nitrate profile, observations in the upper 300 dbar were binned at 5 dbar intervals, and the resulting binned profile was smoothed using a centered five-bin rolling median. The primary nitracline depth was defined as the depth of the maximum positive vertical nitrate gradient within 20–250 dbar, calculated from the smoothed nitrate profile. The nitracline depth should therefore be interpreted as an operational gradient-maximum depth diagnosed from the smoothed nitrate profile. Gradients were evaluated only where adjacent valid bins were separated by no more than 15 dbar.

A nitracline diagnosis was considered successful only when the profile satisfied minimum data-coverage and nitrate-structure criteria. Specifically, profiles were required to contain at least 10 valid nitrate bins, span at least 100 dbar vertically, and show

https://doi.org/10.5194/egusphere-2026-3910
Preprint. Discussion started: 21 July 2026

an increase of at least 1.0 µmol kg^{-1} from the near-surface layer (0–20 dbar) to the deeper layer (200–300 dbar). Profiles were also required to have a maximum positive nitrate gradient of at least 0.005 µmol kg^{-1} $dbar^{-1}$. Profiles that did not satisfy these criteria were excluded from the nitracline-context analysis.

The diagnosed nitracline depth was not used to define the Coupled, Chl deeper, or Chl shallower classes. Instead, nitracline depth was compared with the independently diagnosed Chl DCM and BBP700 maximum depths after profile classification, allowing the nutrient-structure context of each displacement class to be evaluated.

2.7 Relative ordering of Chl DCM, BBP700 maximum, and nitracline

The relative vertical ordering of the Chl DCM, BBP700 maximum, and nitracline was evaluated only for profiles with a successful nitracline diagnosis. For each profile, the nitracline depth was compared with the independently diagnosed Chl DCM and BBP700 maximum depths. The nitracline was classified as shallower than both optical maxima, located between the two optical maxima, or deeper than both optical maxima according to its position relative to the shallower and deeper of the Chl DCM and BBP700 maximum.

To examine how these relative positions varied within each displacement class, profiles were grouped into the Coupled, Chl deeper, and Chl shallower classes defined in Sect. 2.3. Within each class, profiles were sorted by Chl DCM depth and divided into 50 equal-rank bins. A smaller number of rank bins than in the Chl composite analysis was used to retain sufficient profiles within each bin for summarizing nitracline-related structure. For each bin, median depths of the Chl DCM, BBP700 maximum, and nitracline were calculated, together with interquartile ranges to summarize within-bin variability.

This analysis was used to assess the nutrient-structure context of the displacement classes after classification. Because the classes were defined solely from Chl DCM and BBP700 maximum depths, the nitracline ordering provides an independent post-classification comparison rather than an input to the class definitions.

3. Results

3.1 Recent expansion of BGC-Argo observations enables basin-scale analysis of Chl–particle vertical structure

The recent expansion of BGC-Argo observations has improved the observational basis for resolving subsurface biogeochemical structure in the North Pacific study domain. Fig. 1 compares the availability of paired Chl–BBP700 observations between a historical baseline period (2010–2019) and the recent main-analysis period (2022–2025) using 2° × 2° grid cells. Cells were categorized according to whether only candidate Chl–BBP700 profiles were present, whether one to two usable paired profiles were available, or whether at least three usable paired profiles were available. The same paired-profile availability was also summarized seasonally to evaluate whether the recent observing network supports analysis across the annual cycle.

https://doi.org/10.5194/egusphere-2026-3910
Preprint. Discussion started: 21 July 2026

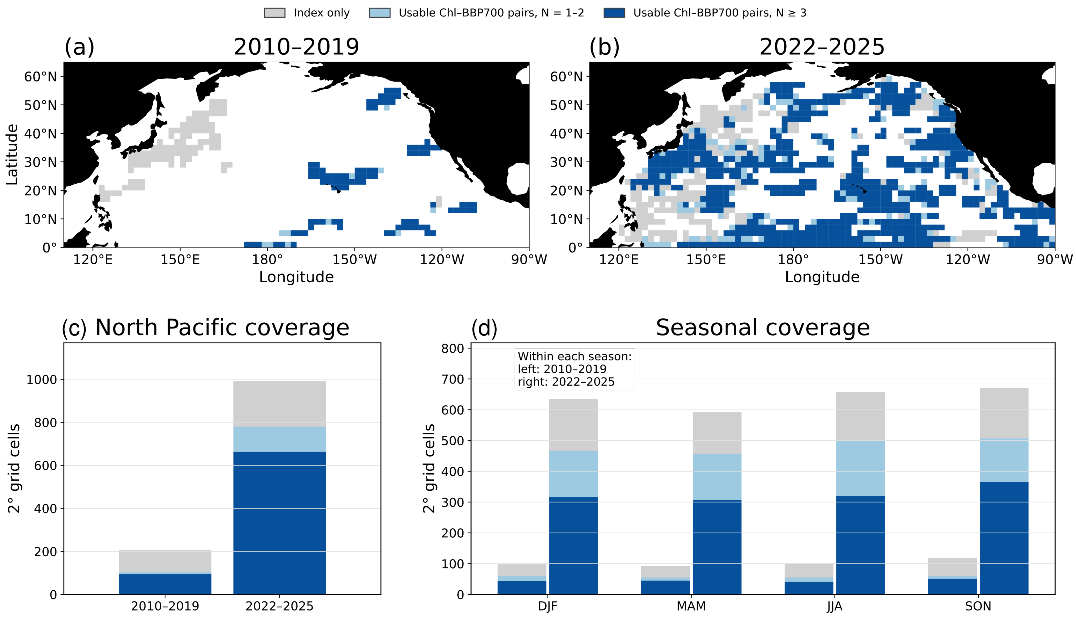

Figure 1. Recent expansion of BGC-Argo paired-profile coverage used to evaluate North Pacific Chl–particle vertical structure. The figure compares profile availability between a historical baseline period (2010–2019) and the recent main-analysis period (2022–2025) within the North Pacific study domain, defined from an initial geographic window of 0–65°N and 110–270°E after applying a Pacific basin mask. The panels summarize the spatial and seasonal availability of usable paired Chl–BBP700 profiles in the historical baseline and recent main-analysis periods. The recent observing network provides the vertically resolved paired in situ profile coverage required to compare operational Chl DCM depth with BBP700 particle-backscattering maximum depth.

This expansion is central to the present analysis because the Chl DCM alone does not necessarily indicate the depth of maximum particle backscattering. The recent availability of usable paired Chl–BBP700 profiles makes it possible to evaluate the relative vertical positions of the Chl DCM and the BBP700 maximum across the North Pacific study domain. Although the observing network remains spatially heterogeneous, the recent paired-profile coverage provides the observational foundation for examining broad regional patterns in Chl–particle vertical structure.

This large, vertically resolved in situ profile set allowed us to examine whether Chl–particle separation appears as **recurring** vertical and spatial structure within naturally variable observations, rather than as isolated profile-level examples.

3.2 Chl–BBP700 displacement reveals structured basin-scale patterns

We next mapped the spatial distributions of Chl DCM depth, BBP700 maximum depth, and their vertical displacement across the North Pacific study domain (Fig. 2). The analysis used 10,801 usable paired Chl–BBP700 profiles aggregated on a 2° × 2° grid, and gridded summary maps were shown only for cells containing at least three usable paired profiles. Vertical displacement was defined as $\Delta z = z(\text{Chl DCM}) - z(\text{BBP700 maximum})$, such that positive values indicate Chl DCMs deeper than the BBP700 maximum and negative values indicate Chl DCMs shallower than the BBP700 maximum. The maps were interpreted as gridded observational summaries of available BGC-Argo profiles, not as interpolated climatological fields.

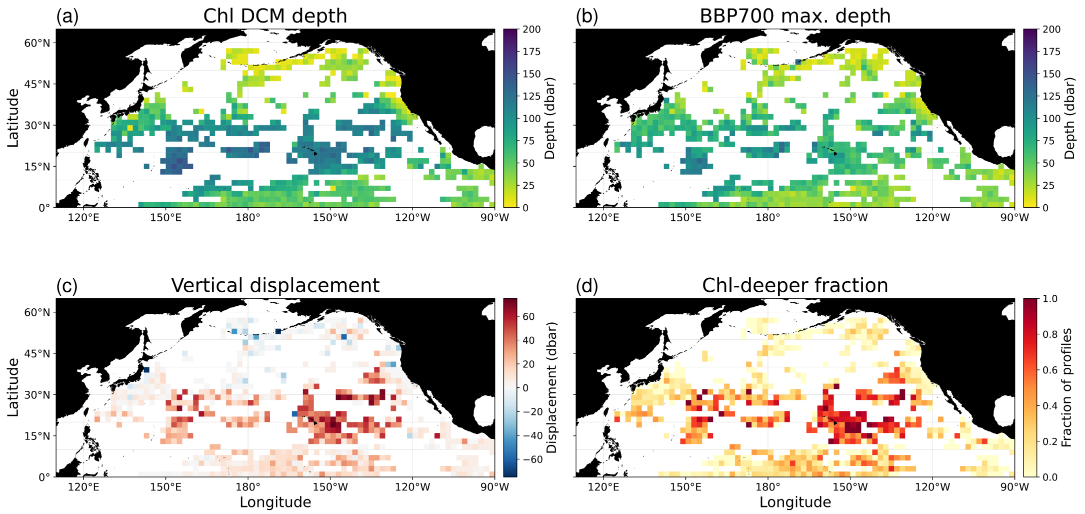

Figure 2. North Pacific relationship between operational Chl DCM depth and BBP700 particle-backscattering maximum depth. Maps summarize Chl DCM depth, BBP700 maximum depth, and vertical displacement, defined as Δz = z(Chl DCM) − z(BBP700 maximum), in 2° × 2° grid cells. The fourth panel shows the fraction of profiles in which the Chl DCM is deeper than the BBP700 maximum, corresponding to positive Δz. Positive Δz indicates profiles in which the Chl DCM lies deeper than the BBP700 maximum, whereas negative Δz indicates profiles in which the Chl DCM lies shallower. Profiles with |Δz| ≤ 25 dbar are classified as Coupled, those with Δz > 25 dbar as Chl deeper, and those with Δz < −25 dbar as Chl shallower. Grid cells with fewer than three usable paired profiles are not shown in the gridded summary maps.

The Chl DCM and BBP700 maximum depths both exhibited broad spatial variability, but their spatial patterns were not identical. Regions with relatively deep Chl DCMs did not always correspond to regions with similarly deep BBP700 maxima, indicating that the subsurface chlorophyll maximum was not uniformly colocated with the particle-backscattering maximum. This mismatch was more clearly expressed by the displacement field, which identified regions where the Chl DCM was deeper or shallower than the BBP700 maximum. These spatially coherent displacement patterns indicate that the Chl DCM cannot be interpreted uniformly as the depth of maximum particle backscattering across the North Pacific study domain.

3.3 Three vertical displacement classes capture distinct Chl–particle vertical structures

To characterize the diversity of Chl–particle vertical relationships at the profile scale, we classified usable paired Chl–BBP700 profiles into three displacement classes based on the relative depths of the Chl DCM and BBP700 maximum (Fig. 3). Coupled profiles were defined by small vertical displacement between the two maxima, whereas Chl deeper and Chl shallower profiles represented cases in which the Chl DCM occurred substantially deeper or shallower than the BBP700 maximum, respectively.

https://doi.org/10.5194/egusphere-2026-3910
Preprint. Discussion started: 21 July 2026

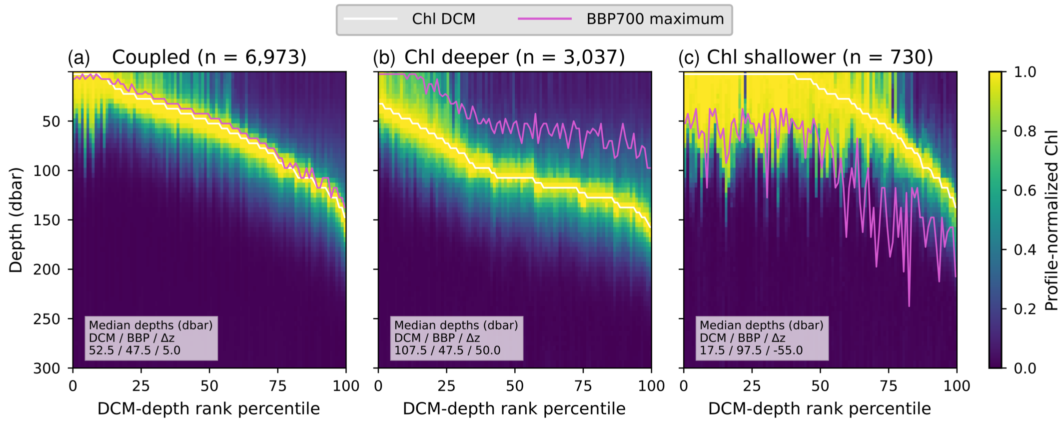

Figure 3. DCM-sorted Chl profile structure for Coupled, Chl deeper, and Chl shallower profiles. Within each displacement class, profiles were sorted by Chl DCM depth and grouped into 100 equal-rank bins. Colors show the median Chl value within each depth and rank bin after normalizing each profile by its own maximum Chl value. Overlaid lines show the unsmoothed bin-wise median depths of the Chl DCM and BBP700 maximum. Sample sizes are shown in the panel titles. This rank-binned view summarizes how Chl vertical structure and the relative positions of the Chl DCM and BBP700 maximum vary within each displacement class.

The three classes exhibited distinct vertical Chl structures in the rank-binned composites. In Coupled profiles, the Chl DCM and BBP700 maximum were located at similar depths, with median depths of 52.5 and 47.5 dbar, respectively, and a median displacement of +5.0 dbar. In Chl deeper profiles, the BBP700 maximum was relatively shallow, with a median depth of 47.5 dbar, whereas the Chl DCM was displaced downward to a median depth of 107.5 dbar, yielding a median displacement of +50.0 dbar. In contrast, Chl shallower profiles showed a shallow Chl DCM and a deeper BBP700 maximum, with median depths of 17.5 and 97.5 dbar, respectively, and a median displacement of −55.0 dbar. These contrasting structures indicate that the Chl DCM occurs within different Chl–particle configurations across profiles, rather than within a single uniform vertical arrangement of chlorophyll and particle-backscattering maxima.

3.4 Displacement classes show coherent basin-scale spatial organization

We next examined whether the three Chl–BBP700 displacement classes were spatially organized across the North Pacific study domain (Fig. 4). The class-fraction analysis used the 10,801 usable paired Chl–BBP700 profiles described above, and gridded summaries were calculated on a 2° × 2° grid. Class-fraction panels were restricted to grid cells with at least three usable paired profiles; this criterion retained 663 grid cells containing 10,630 profiles. Cells with fewer than three profiles were left blank to avoid interpreting class fractions in grid cells represented by only one or two profiles.

https://doi.org/10.5194/egusphere-2026-3910
Preprint. Discussion started: 21 July 2026

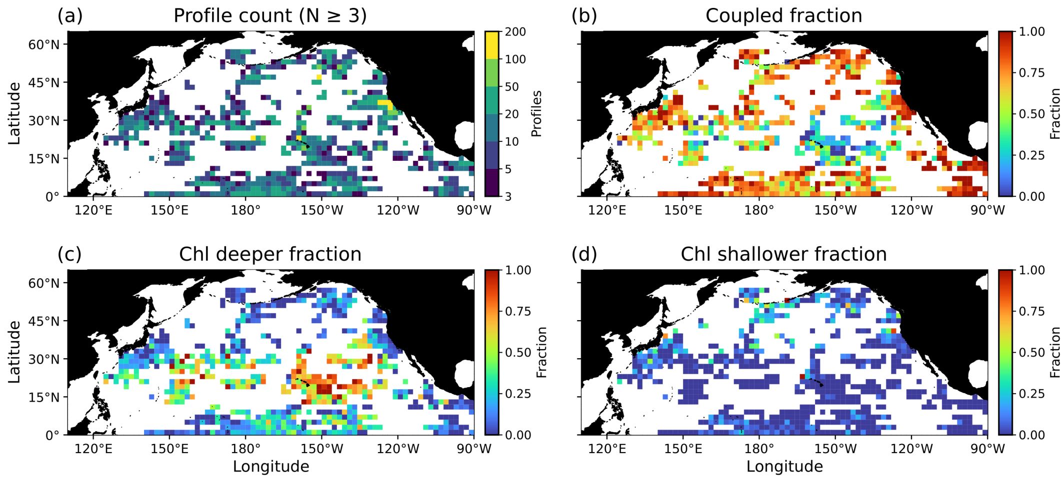

Figure 4. Spatial distribution of Chl–BBP700 displacement classes across the North Pacific study domain. The figure summarizes the number of usable paired Chl–BBP700 profiles and the fractions of Coupled, Chl deeper, and Chl shallower profiles in 2° × 2° grid cells. Class-fraction maps are shown only for grid cells with at least three usable paired profiles, retaining 663 grid cells and 10,630 profiles in the gridded summary. The maps represent cell-wise observational summaries of available BGC-Argo profiles and are not spatially interpolated fields. The coherent geographical patterns suggest basin-scale organization of Chl–BBP700 coupling and decoupling rather than purely random profile-level variability.

The class-fraction maps indicated that the three displacement classes were not distributed uniformly across the basin. Instead, the relative occurrence of Coupled, Chl deeper, and Chl shallower profiles varied geographically, showing that the vertical relationship between chlorophyll and particle-backscattering maxima has coherent regional structure. This spatial organization indicates that the displacement classes are not isolated profile-level occurrences, but recurring Chl–particle configurations observed across multiple parts of the basin. The spatial patterns in class fractions therefore extend the profile-level structures shown in Fig. 3 to the basin scale.

3.5 Nitracline context of Chl–particle vertical displacement

Finally, we examined how the three Chl–BBP700 displacement classes were positioned relative to the nitracline (Fig. 5). The nitracline was not used to define the displacement classes; instead, it was used as an independent nutrient-structure context for profiles in which nitracline depth could be diagnosed. This analysis was based on 9,402 profiles with successful nitracline diagnosis, corresponding to the subset of usable paired Chl–BBP700 profiles for which nitracline depth could be diagnosed.

https://doi.org/10.5194/egusphere-2026-3910
Preprint. Discussion started: 21 July 2026

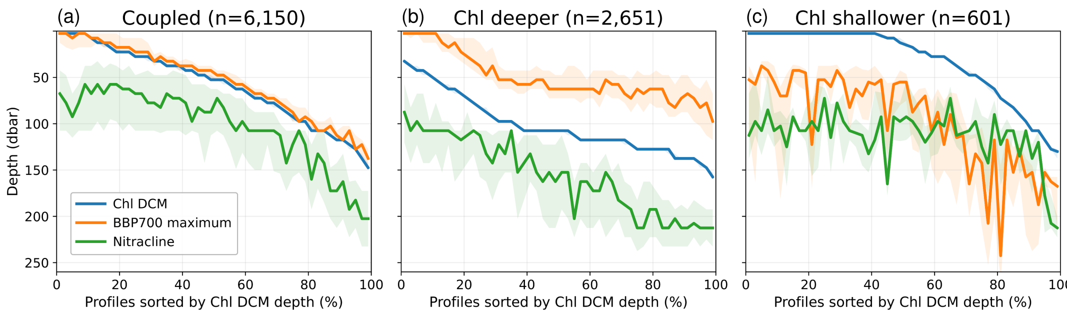

Figure 5. Nitracline context of Chl DCM and BBP700 maximum vertical ordering. Profiles were separated into Coupled, Chl deeper, and Chl shallower classes based on the vertical displacement between the Chl DCM and the BBP700 maximum, and were then sorted within each class by Chl DCM depth. Each class was divided into 50 equal-rank bins. Lines show bin-wise median depths of the Chl DCM, BBP700 maximum, and nitracline, and shaded bands show interquartile ranges. The nitracline was diagnosed independently from nitrate profiles as the depth of the maximum positive vertical nitrate gradient. Sample sizes are 6,150 for Coupled, 2,651 for Chl deeper, and 601 for Chl shallower profiles.

Thus, the class counts in the Chl–BBP700 profile-structure analysis refer to the full paired-profile population, whereas the nitracline-ordering analysis uses only the subset of profiles with successful nitracline diagnosis. In the final nitracline-context subset, the class sample sizes were 6,150 Coupled profiles, 2,651 Chl deeper profiles, and 601 Chl shallower profiles.

The relative positions of the Chl DCM, BBP700 maximum, and nitracline differed among the three displacement classes. In Coupled profiles, the Chl DCM and BBP700 maximum were located at similar depths, while the nitracline was generally deeper than both optical maxima. In Chl deeper profiles, the BBP700 maximum was relatively shallow, the Chl DCM was displaced downward, and the nitracline tended to occur still deeper. In Chl shallower profiles, the Chl DCM was shallow, whereas the BBP700 maximum occurred deeper and was often closer to the nitracline. These results indicate that Chl–particle displacement classes are embedded in different nutrient-structure contexts, even though the classes themselves were defined solely from the relative depths of the Chl DCM and BBP700 maximum.

4. Discussion

4.1 DCM–BBP700 displacement reveals multiple DCM structure types

Our results do not imply that Chl–particle separation is a newly discovered phenomenon. Instead, they show how this previously recognized separation appears within nature North Pacific BGC-Argo observations: as recurring Chl–BBP700 vertical configurations with coherent spatial distributions and distinct nitracline contexts.

The vertical displacement between the Chl DCM and the BBP700 maximum shows that North Pacific Chl DCMs do not represent a single uniform vertical bio-optical structure (Figs. 2 and 3). A central result of this study is not only that the two maxima can occur at different depths, but that their relative depth provides a useful observational diagnostic for distinguishing Chl maxima that are closely aligned with particle-backscattering structure from those that are vertically decoupled from it. Because Δz was defined as z(Chl DCM) − z(BBP700 maximum), positive values identify profiles in which the Chl DCM lies deeper than the BBP700 maximum, whereas negative values identify profiles in which the Chl DCM lies shallower. This definition provides a simple way to describe the vertical ordering of the two optical features without assuming that they represent the same bio-optical structure.

This displacement-based view directly addresses the interpretive ambiguity of subsurface Chl maxima. A Chl maximum can reflect increased phytoplankton amount, increased cellular pigment content associated with photoacclimation, or both (Fennel and Boss, 2003; Cullen, 2015; Cornec et al., 2021). BBP700 provides an independent optical particle-backscattering signal

https://doi.org/10.5194/egusphere-2026-3910
Preprint. Discussion started: 21 July 2026

with which to evaluate whether the Chl maximum is accompanied by a corresponding particle-backscattering maximum (Barbieux et al., 2018; Cornec et al., 2021). Thus, the main value of the Chl–BBP700 comparison is that it treats the Chl DCM as an operational Chl feature whose relation to particle-associated optical structure must be evaluated explicitly, rather than inferred from Chl alone.

4.2 Coupled and decoupled DCM structures

Coupled profiles represent the clearest case in which the Chl DCM is accompanied by a nearby BBP700 particle-backscattering maximum. This was the most frequent displacement class. The close vertical alignment in this class supports the interpretation that, for a large fraction of profiles, the subsurface Chl maximum is associated with a particle-backscattering maximum at a similar depth. This does not require treating BBP700 as a direct measure of phytoplankton biomass. Rather, it identifies cases in which the Chl maximum and an independent particle-backscattering maximum occur together in the vertical profile.

Chl deeper profiles show a different structure, in which the Chl maximum occurs deeper than the BBP700 maximum. This separation indicates that the deep Chl maximum is not matched by a particle-backscattering maximum at the same depth. Such a structure is consistent with a stronger contribution of photoacclimation or pigment adjustment to the Chl maximum, because Chl can increase with depth even when particle backscattering does not show a corresponding maximum. However, the displacement alone does not identify photoacclimation as the sole process involved. Accordingly, Chl deeper profiles are best described as a decoupled Chl–particle optical structure in which the Chl maximum does not coincide with the particle-backscattering maximum.

Chl shallower profiles demonstrate that Chl–BBP700 decoupling is not unidirectional. This less frequent class showed the reverse configuration, with a shallow Chl maximum and a deeper BBP700 maximum. Because this class is less frequent than the Coupled and Chl deeper classes, it should be interpreted cautiously. Nevertheless, it is important because it shows that Chl–BBP700 mismatch is not simply a matter of Chl maxima being deeper than particle-backscattering maxima; the reverse configuration also occurs and contributes to the diversity of DCM structures in the North Pacific.

4.3 Spatial organization of Chl–BBP700 displacement regimes

The displacement classes are spatially organized across the North Pacific, suggesting basin-scale organization of Chl–BBP700 coupling and decoupling rather than purely random profile-level variability. Class fractions were calculated on a 2° × 2° grid using the main paired Chl–BBP700 profile population, with class-fraction maps restricted to grid cells containing at least three usable paired profiles. The relative occurrence of Coupled, Chl deeper, and Chl shallower profiles varied geographically, showing that the vertical relationship between chlorophyll and particle-backscattering maxima has coherent basin-scale structure.

This spatial coherence supports the interpretation of the three classes as recurring bio-optical structure types, even though they are defined using fixed displacement thresholds. The profile-level analysis shows that the classes differ in vertical structure, while the spatial analysis shows that these differences are organized across the basin (Figs. 3 and 4). At the same time, the maps should be interpreted as broad observational patterns rather than as sharply bounded provinces. This interpretation does not depend on predefined western, central, or eastern North Pacific boxes. Instead, the spatial distribution is best viewed as evidence that Chl–BBP700 displacement varies systematically across the North Pacific as part of broader differences in upper-ocean bio-optical structure.

4.4 Nitracline depth as nutrient-structure context

Nitracline depth provides an independent nutrient-structure context for the displacement classes, rather than a criterion used to define them. The Coupled, Chl deeper, and Chl shallower classes were defined solely from the relative depths of the Chl DCM and the BBP700 maximum. Nitracline diagnosis was then applied as a post-classification analysis, yielding 9,402

https://doi.org/10.5194/egusphere-2026-3910
Preprint. Discussion started: 21 July 2026

profiles with successful nitracline diagnosis (Fig. 5). This separation between class definition and nitracline diagnosis is important because it prevents the nutrient field from being built into the class definitions and allows nitracline depth to be used as an independent context for interpreting the vertical ordering of the optical maxima.

The vertical ordering of the nitracline relative to the two optical maxima differed among the displacement classes, reinforcing that Chl–BBP700 displacement and nutrient structure are related but not identical diagnostics. In Coupled and Chl deeper profiles, the nitracline was generally deeper than both optical maxima, whereas in Chl shallower profiles the deeper BBP700 maximum occurred closer to the nitracline depth range. These patterns indicate that nitracline depth provides useful nutrient-structure context for the vertical structure of the classes, especially for cases in which the BBP700 maximum lies deeper than the Chl maximum. However, nitracline depth should not be interpreted as a criterion for class membership. The classification is based on Chl–BBP700 displacement, while the nitracline describes the nutrient-structure setting in which that displacement occurs.

4.5 Implications for Chl-only, satellite, and model interpretations

These results highlight a general limitation of Chl-only interpretations: a subsurface Chl maximum cannot automatically be assumed to mark the particle-backscattering maximum (Cullen, 2015; Cornec et al., 2021; Figs. 2–5). The Coupled class shows that Chl maxima are often accompanied by nearby BBP700 maxima, whereas the Chl deeper and Chl shallower classes show that this alignment is not universal. Chl vertical structure alone therefore provides an incomplete basis for inferring particle-associated optical structure.

For satellite and model applications, the implication is interpretive rather than corrective. Surface-focused observations do not resolve the subsurface vertical arrangement of Chl and particle-backscattering maxima, and modeled Chl maxima do not necessarily imply that particle-related optical structure is reproduced at the same depth. Recent BGC-Argo studies have demonstrated the value of resolving subsurface Chl structure across broad ocean regions and have highlighted the expanding observational basis for interpreting Chl variability in the western North Pacific (Yasunaka et al., 2022; Hayashida et al., 2025). Building on this progress, the present results support interpreting Chl-based vertical structure together with independent particle-related optical proxies whenever possible. This should be read as guidance for interpreting Chl-based structure, not as a direct assessment of satellite products or model performance.

4.6 Limitations and concluding perspective

The displacement framework is observationally useful, but its interpretation is bounded by the optical-proxy nature of both Chl fluorescence and BBP700. Chl fluorescence is affected by phytoplankton amount and cellular pigment content associated with photoacclimation, whereas BBP700 represents a particle-backscattering signal and is not a direct measurement of phytoplankton biomass (Cullen, 2015; Cornec et al., 2021). Nitracline context was available only for the subset of paired Chl –BBP700 profiles with successful nitracline diagnosis, and nitracline detection depends on nitrate-profile coverage and the adopted gradient-based criteria. In addition, BGC-Argo sampling is not spatially uniform, so spatial patterns should be interpreted as basin-scale observational structures rather than exhaustive maps of all North Pacific conditions. The observed frequency of Chl shallower profiles should also be interpreted in light of uneven sampling of seasonally dynamic or bloom-influenced regions.

Despite these limitations, comparing Chl DCM depth with BBP700 maximum depth provides a consistent observational basis for describing coupled and decoupled DCM structures across the North Pacific. The three displacement classes are supported by the depth relationship between the two maxima, their distinct vertical profile structures, their spatial organization, and their nitracline context (Figs. 2–5). Rather than assigning a single mechanism to every DCM, this analysis shows that Chl DCMs differ systematically in their relationship to particle-backscattering structure. In this way, the known ambiguity of Chl maxima

https://doi.org/10.5194/egusphere-2026-3910
Preprint. Discussion started: 21 July 2026

is expressed in mature BGC-Argo observations as basin-scale organization of coupled and decoupled Chl–particle regimes in the North Pacific.

This displacement framework provides an observational basis for evaluating when a Chl DCM is accompanied by particle-backscattering structure and when it is vertically separated from it. Its value is therefore not limited to classifying North Pacific DCMs, but extends to the interpretation of Chl vertical structure in relation to particle-related optical structure and nutrient context. This perspective is relevant for Chl-only, satellite, and model-based interpretations, because surface Chl or Chl vertical structure alone cannot determine whether a subsurface Chl maximum is associated with a particle-backscattering maximum.

At the same time, the present analysis does not directly identify the physiological or ecological processes that generate each displacement class. Future work should link this displacement framework to seasonal evolution, other ocean basins, phytoplankton community composition, particulate carbon, export-related particle fluxes, and model output. Such extensions would help determine how Chl–particle displacement relates to ecosystem structure and carbon cycling, and would move BGC-Argo DCM observations beyond the description of Chl maxima toward a broader diagnosis of upper-ocean ecological, optical, and biogeochemical structure.

Code availability

Public Python scripts for validating the processed source tables and generating reproducibility-check diagnostic figures are available in the Zenodo reproducibility package. The scripts use package-relative paths and do not depend on private paths. The code has been tested within the repository staging package: 14 CSV source tables were loaded successfully and 5 simplified diagnostic figures were generated.

The public code archive is available as part of the reproducibility package at Zenodo (Hashioka and Aita, 2026) with DOI: 10.5281/zenodo.20873450 and URL: https://doi.org/10.5281/zenodo.20873450.

Data availability

Original BGC-Argo profile data are publicly available from the Argo Global Data Assembly Centres through the Coriolis and US-GODAE GDACs (Argo, 2000). These data were collected and made freely available by the International Argo Program and the national programs that contribute to it. The Argo Program is part of the Global Ocean Observing System. This study does not redistribute raw BGC-Argo NetCDF profile files.

The processed figure source tables, profile-level diagnostic subsets, and gridded summary products supporting the manuscript are available in the public data repository. The repository includes processed Chl DCM and BBP700 maximum diagnostics, Chl–BBP700 displacement classes, nitracline summary products, gridded class-fraction products, and source tables for Figs. 1–5. The processed data archive is available as part of the reproducibility package at Zenodo (Hashioka and Aita, 2026) with DOI: 10.5281/zenodo.20873450 and URL: https://doi.org/10.5281/zenodo.20873450.

Author contributions

TH designed the study, processed the BGC-Argo data, developed the diagnostic framework, performed the analysis, produced the figures, interpreted the results, and wrote the original draft. MNA contributed to the scientific framing, interpretation of the North Pacific biogeochemical context, funding acquisition, and manuscript review and editing. Both authors discussed the results and approved the final manuscript.

https://doi.org/10.5194/egusphere-2026-3910
Preprint. Discussion started: 21 July 2026

Competing interests

The authors declare that they have no conflict of interest.

Acknowledgements

We thank the BGC-Argo and Argo communities, float operators, data centres, and quality-control teams for making the observational data publicly available.

Financial support

This study was supported by institutional funding from the Japan Agency for Marine-Earth Science and Technology (JAMSTEC) and by the Japan Science and Technology Agency (JST) CREST program through the project "Carbon cycle and Lower trophic level oceanic organisms Investigation for Future Environments (C-LIFE)" (grant no. JPMJCR24J1).

References

Argo: Argo float data and metadata from Global Data Assembly Centre (Argo GDAC), SEANOE, https://doi.org/10.17882/42182, 2000.

Barbieux, M., Uitz, J., Bricaud, A., Organelli, E., Poteau, A., Schmechtig, C., Gentili, B., Obolensky, G., Leymarie, E., Penkerc'h, C., D'Ortenzio, F., and Claustre, H.: Assessing the variability in the relationship between the particulate backscattering coefficient and the chlorophyll a concentration from a global Biogeochemical-Argo database, J. Geophys. Res.-Oceans, 123, 1229–1250, https://doi.org/10.1002/2017JC013030, 2018.

Cornec, M., Claustre, H., Mignot, A., Guidi, L., Lacour, L., Poteau, A., D'Ortenzio, F., Gentili, B., and Schmechtig, C.: Deep chlorophyll maxima in the global ocean: occurrences, drivers and characteristics, Global Biogeochem. Cy., 35, e2020GB006759, https://doi.org/10.1029/2020GB006759, 2021.

Cullen, J. J.: Subsurface chlorophyll maximum layers: enduring enigma or mystery solved?, Annu. Rev. Mar. Sci., 7, 207–239, https://doi.org/10.1146/annurev-marine-010213-135111, 2015.

Fennel, K. and Boss, E.: Subsurface maxima of phytoplankton and chlorophyll: steady-state solutions from a simple model, Limnol. Oceanogr., 48, 1521–1534, https://doi.org/10.4319/lo.2003.48.4.1521, 2003.

Hashioka, T. and Aita, M. N.: Data and code for "Chlorophyll–particle backscattering displacement reveals multiple deep chlorophyll maximum structures in the North Pacific", Zenodo [data set and code], https://doi.org/10.5281/zenodo.20873450, 2026.

Hayashida, H., Strutton, P. G., Hashihama, F., Horimoto-Miyazaki, N., Katano, T., and Yasui-Tamura, S.: Status and prospects of biogeochemical Argo observations of chlorophyll-a in the northwest Pacific, J. Oceanogr., 81, 289–299, https://doi.org/10.1007/s10872-025-00750-2, 2025.

Yasunaka, S., Ono, T., Sasaoka, K., and Sato, K.: Global distribution and variability of subsurface chlorophyll a concentrations, Ocean Sci., 18, 255–268, https://doi.org/10.5194/os-18-255-2022, 2022.